Investigation of Excited States of Helium Atoms in a Stationary PIG-Discharge *

H. W. DRAWIN

Association Euratom-CEA Département de la Physique du Plasma et de la Fusion Contrôlée
Centre d'Etudes Nucléaires, Fontenay-aux-Roses (France)

and

F. KLAN and H. RINGLER

Institut für Plasmaphysik G.m.b.H., Garching (Germany)

(Z. Naturforsch. **26 a**, 186—197 [1971]; received 25 November 1970)

Spectral line intensities emitted by a quiescent PIG-discharge have been measured and the population densities up to a principal quantum number $n = 24$ have been derived from them. The experimentally determined population densities have been compared with theoretical ones calculated on the basis of a collisional-radiative model in which one accounts for electron and atom collisions. It is shown that even in the case of different electron and atom temperatures, T_e and T_a, an evaluation of the Boltzmann plot at medium and moderately high quantum numbers always leads to the electron temperature, whereas the Saha-Eggert equation for the same states may yield incorrect electron densities. The theoretical calculations predict an inflection of the slope of the Boltzmann plot from T_e to T_a for very highly excited states. For the plasma parameters under which the PIG-discharge was operated ($n_e \cong 2.5 \times 10^{12}$ cm^{-3}, $T_e \cong 1200$°K, $n_0 \cong 1.5 \times 10^{15}$ cm^{-3}, $T_a \cong 300$°K) the change of the slope should become visible for states having principal quantum numbers $n > 18$. Due to the large experimental error bars it was not possible to check this behaviour.

A. Introduction

In weakly ionized gases the population densities of the higher excited states of atoms and ions are usually assumed to be in equilibrium with the free electrons. This means that the population densities of these states are only governed by collisions with free electrons, radiation processes have no influence upon the level populations. For a Maxwellian velocity distribution of the electrons the population densities will show a Saha-Boltzmann distribution, at least for levels lying above a certain critical principal quantum number $n_{cr} = i$ which may be estimated by comparing the different rates leading to excitation and de-excitation of the various levels. For a low temperature recombining afterglow plasma the critical quantum number has been found to be [1]

$$n_{cr} = i \cong \left(\frac{E_0}{k\,T_e}\right)^{1/2} \qquad (1)$$

where $k\,T_e$ is the electron temperature in eV and E_0 is some equivalent ionization energy ($E_0 = 13.6$ eV in the hydrogenic approximation). Relation (1) agrees with the results of other authors [2–5] within a factor of approximately two. In deriving Eq. (1) the assumption was made that only electronic collisions are effective and that the effect of heavy particle collisions on the population densities can be neglected.

Using refined cross sections and evaluating the collisional and radiative terms more precisely one obtains instead of Eq. (1) a relation between the electron density n_e, the electron temperature T_e and the critical quantum number i, which permits the calculation of i when n_e and T_e are known [6–8]. The corresponding formula writes [7,8]

$$n_e = 7.4 \times 10^{18}\, \frac{Z^4}{i^{17/2}} \left(\frac{k\,T_e}{Z^2\, E_1^H}\right)^{1/2} \times \begin{cases} \Phi_1(u_{i\to i-1})\ \text{cm}^{-3} & \text{for atoms } (Z=1)\,, \\ \Phi_2(u_{i\to i-1})\ \text{cm}^{-3} & \text{for ions } (Z>1)\,. \end{cases} \qquad (2)$$

* Work performed under association contracts with Euratom, Bruxelles.

Reprint requests to: Dr. H. W. DRAWIN, Association Euratom-CEA, Fusion Contrôlée, F-92 *Fontenay-aux-Roses* (France) B.P.No. 6, or to Dr. H. RINGLER, Institut für Plasmaphysik G.m.b.H., *D-8046 Garching* (Germany).

[1] E. HINNOV and J. G. HIRSCHBERG, Phys. Res. **125**, 795 [1962].
[2] S. BYRON, R. C. STABLER and P. I. BARTZ, Phys. Rev. Letters 8, 376 [1962].
[3] B. MAKIN and J. C. KECK, Phys. Rev. Letters **11**, 281 [1963].
[4] H. W. DRAWIN, Z. Physik **186**, 99 [1965].
[5] B. P. CURRY, Phys. Rev. A, **1**, 166 [1970].
[6] H. R. GRIEM, Plasma Spectroscopy. McGraw Hill, New York 1964.
[7] H. W. DRAWIN, Z. Physik **228**, 99 [1969].
[8] H. W. DRAWIN, Article in: Ergebnisse der Plasmaphysik und Gaselektronik. Herausg. R. ROMPE and M. STEENBECK; German edition: Vol. III, Akademie Verlag, Berlin 1971; English Edition: Vol I. Gordon & Breach, New York 1971.

The functions $\Phi_1(x)$ and $\Phi_2(x)$ account for the special structure of the excitation cross sections with energy*. For sufficiently excited states one can use for $\Phi_1(x)$ the following formula:

$$\Phi_1(x) \cong \frac{(1+x)}{\left[\frac{1}{20+x} + \ln\left(1.25\left(1+\frac{1}{x}\right)\right)\right]}. \quad (3a)$$

Further

$$u_{n\to n-1} \cong 2\,E_1^{\mathrm{H}}/k\,T_e\,n^3\,, \quad (3b)$$

$E_1^{\mathrm{H}} = 13.6\,\mathrm{eV}$ (ionization energy of atomic hydrogen). (3c)

Quantitative spectroscopic investigation of different afterglow plasmas[1,10,11] have shown that there is in fact a Saha-Boltzmann distribution (relative to the electron temperature) for all excited states having principal quantum numbers n around or larger than $n_{\mathrm{cr}} = i$. This has been proved to be true up to $n = 13$, and one would expect that the higher the quantum number n the better the Saha-Boltzmann equilibrium should be established, provided that only electronic collision processes are of importance.

However, when the electron density, n_e, is much smaller than the density of the neutral atoms, n_0, atom-atom collisions may be as efficient as electron-atom and electron-ion collisions in populating excited states. When the gas temperature, T_a, is different from the electron temperature, T_e, a Boltzmann plot of the population densities will give neither T_a nor T_e but some intermediate temperature T_n which additionaly will depend on the principal quantum number n at which the slope (which serves for calculating the temperature) has been determined.

The higher n the more will T_n approach T_a, provided neutral atoms are sufficiently abundant so that atomic collisions can become important compared to electronic collisions[12,13]. It is evident that T_n depends on the ratio n_e/n_0 and on the ratio of the collision integrals for electronic and atomic collisions.

By comparing the de-excitation rates between highly excited states due to electronic and atomic collisions it is possible to formulate a condition which must be fulfilled in order to ensure that all excited states of principal quantum number n lying above some critical quantum number j are populated by atomic collisions, i.e. that they follow the gas temperature T_a on a Boltzmann plot. The necessary condition is[7,8]

$$\frac{n_n\,n_0\langle\sigma_a v_a\rangle_{n\to n-1}}{n_n\,n_e\langle\sigma_e v_e\rangle_{n\to n-1}} \gg 1 \quad (4)$$

where n_n denotes the population density of state n.

When in condition (4) the sign of inequality ($\gg 1$) is replaced by the sign of equality ($=1$) one gets a condition for the state of critical quantum number j that just suffers an equal number of electronic and atomic de-excitation collisions. Using appropriate approximations for the cross sections one obtains as a condition for j the following analytical expression:

$$\frac{2}{\sqrt{2}}\frac{n_0}{n_e}\frac{m_e}{m_H}\left(\frac{m_e}{m_a}\right)^{1/2}\left(\frac{T_a}{T_e}\right)^{1/2}\frac{k\,T_e}{E_1^{\mathrm{H}}} \times\left(1+\frac{k\,T_a}{2\,E_1^{\mathrm{H}}}j^3\right)j^3\,\Phi_1(u_{j\to j-1}) = 1 \quad (5)$$

where m_e, m_H and m_a are respectively masses of electrons, hydrogen atoms and the gas atoms of which the gas under investigation is composed. $\Phi_1(x)$ has the same meaning as in (2).

Only for states having principal quantum numbers $n > j$ one can expect an inflection of the Boltzmann plot from T_e to T_a. For all states with $n < j$ the Boltzmann plot will give T_e provided the corresponding levels are in partial L.T.E. with respect to the free electrons. Under almost all experimental conditions $j > i$ holds, due to the structure of Eqs. (2) and (5).

Putting into Eqs. (2) and (5) the following numerical parameters for a low-temperature helium plasma:

$$n_e = 1\times10^{12}\,\mathrm{cm}^{-3},\quad T_e = 1.2\times10^3\,^\circ\mathrm{K}\,,$$
$$n_a = 1\times10^{15}\,\mathrm{cm}^{-3},\quad T_a = 300\,^\circ\mathrm{K}\,,\quad m_a = 4\,m_H$$

one obtains $j \cong 17$ and $i \cong 5$, whereas Eq. (1) gives $i \cong 11$. The parameters chosen correspond approximately to those found in our discharge.

* Numerical values of the functions $\Phi_1(x)$ and $\Phi_2(x)$ may be found in refs. [4,8,9].

[9] H.W. Drawin, in: Invited lectures of V-th Symposium and Summer School on the Physics of Ionized Gases S.P.I.G. Hercegnovi 1970, Edit. B. Navinsek, Institute Josef Stefan, Ljubljana (Jugoslavia).

[10] F. Robben, W. B. Kunkel and L. Talbot, Phys. Rev. **132**, 2363 [1963].

[11] L. C. Johnson and E. Hinnov, Phys. Rev. **187**, 143 [1969].

[12] H. Drawin, Z. Naturforsch. **25a**, 145 [1970].

[13] C. B. Collins, Phys. Rev. **186**, 113 [1969].

In order to check the theoretically predicted different behaviour of the population densities with respect to the electron and gas temperatures for medium and high principal quantum numbers a detailed experimental and theoretical investigation of a steady-state helium plasma has been undertaken. The aim of the present work is threefold: 1. We want to show that the evaluation of the population densities of medium and high principal quantum numbers n ($j \geqq n \geqq i$) always leads to the electron temperature independent from atom density and gas temperature. — 2. We want to show that the application of the usual Saha-Eggert equation for highly excited states becomes dubious in the case of high gas densities n_0 and different electron and gas temperatures. — 3. To look for the influence of the gas temperature on the population densities of very highly excited states (i.e. for quantum numbers $n > j$) and eventually to show that equipartionning is due to atom-atom collisions.

B. Description of the Discharge Apparatus

The plasma has been produced in a modified PIG discharge[14,15] which could be operated in an extremely stable mode. Because of its stability the discharge is called "quiescent PIG" (Q-PIG).

The Q-PIG discharge differs from other PIG-discharges in that the electrodes are concentrated very close to each other as shown in Fig. 1. The

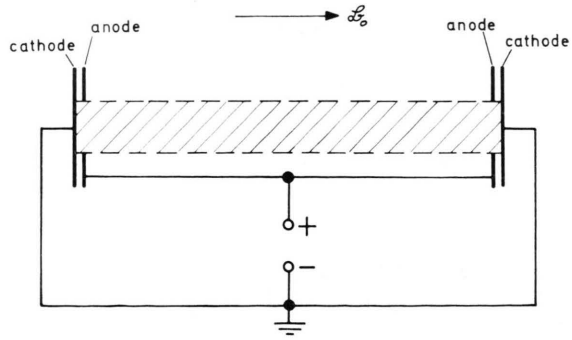

Fig. 1. Arrangement of electrodes in the Q-PIG device. B_0 denotes the confining magnetic field.

anode of each electrode system is a ring shaped aluminium disc of 10 mm thickness and an inner diameter of 5 cm, the cathode is a plane disc of molybdenum mounted on a complex supporting system involving water cooling, vacuum tight connections etc.; for more details the reader is referred to [14]. The distance between each anode and its cathode is only 1 mm. Both anodes and both cathodes are connected electrically with each other. If magnetic field and gas pressure are kept at appropriate values, a discharge may be operated by means of an electric potential across the anodes and cathodes. At certain values of magnetic field and gas pressure the plasma is very stable and quiescent and well confined within a column as indicated in Fig. 1 by the shaded region. The length of the plasma column is 50 cm, its diameter about 5 cm. Some other details are (typically): Magnetic field strength 400 Gauss, gas pressure (He) 50 m Torr (equivalent to a number density $n_0 = 1.4 \times 10^{15}$ cm^{-3} at $T_a = 300$ °K), operating voltage 500 V, discharge current 150 mA.

The technical arrangement of the vacuum tube and the electrode systems is shown in Fig. 2. The central part is an aluminium ring having four ports one of which is usually connected with the pumping system. Two other ports which are opposite to each other were closed with optical windows made of quartz, since the helium spectrum extends well to the UV region. The last port served for inserting probes into the vacuum chamber. The central ring has a thickness of 100 mm and an inner diameter of 102 mm. Two glass tubes of the same inner diameter are connected to the central ring each of which is 30 cm long. The ends of these tubes are closed with the electrode systems. The whole discharge tube is mounted in such a way that two packets of watercooled coils can be moved from each side over the vessel in order to obtain a homogeneous magnetic field.

After the discharge was operated a few hours, excellent stability and reproducibility is reached. Before filling the tube with helium, a residual pressure of $2 \cdots 3 \cdot 10^{-6}$ Torr can be obtained without baking. In the experiments being described here a cooling trap filled with liquid nitrogen was always used in order to improve the vacuum and to prevent contaminations by molecular gases or vapours. Previous spectroscopic investigations had shown that the helium spectrum emitted by the Q-PIG is relatively clean, the only appreciable contamination being due to atomic hydrogen. Therefore, even ex-

[14] F. KLAN, Report IPP 3/92, Garching, April 1969.

[15] F. KLAN, Z. Naturforsch. **25a**, 623 [1970].

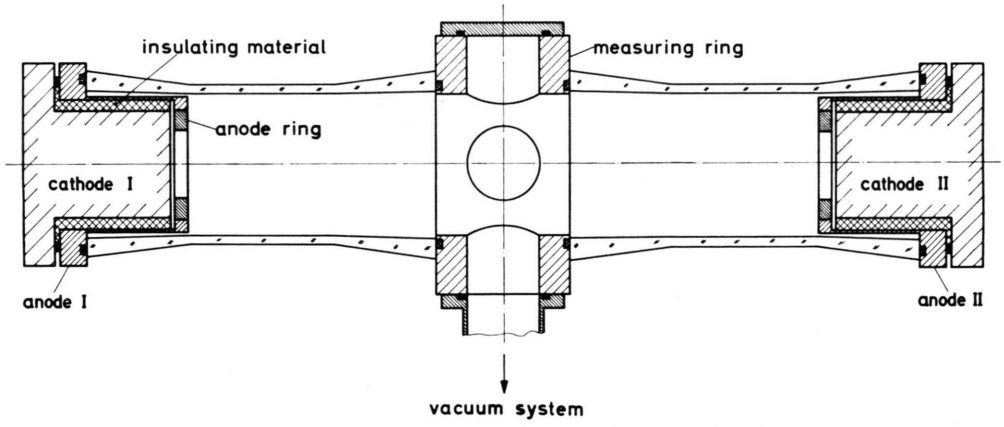

Fig. 2. Longitudinal cross section of the discharge chamber.

posure times of several hours could be used which are necessary to detect the very high series members.

It is to be noted that the electron temperature in the Q-PIG is as low as some tenths of an eV, whereas the electron density is of the order of 10^{12} to 10^{13} cm^{-3}. These values are similar to those in the after-glow plasmas referred to in [1,10,11]. In addition, the number density of the neutral atoms, n_0, is high compared to the electron density, n_e. Thus, neutral atoms may influence the population densities of the very highly excited levels if $T_e \neq T_a$. Since the mean free path of the atoms in the ground state is large one can assume that the strong collision coupling with the walls holds the gas temperature at wall temperature, hence $T_a \cong T_{wall} \cong 300\,°K$. Observation of spectral lines originating from very highly excited states ($n > 17$ to 20) should, thus, lead to temperatures which are different from those originating from medium excited states with $n < 17$.

C. Investigation of Relative Intensities of the Spectral Lines

The purpose of this investigation was to decide whether or not the population densities of the very highly excited states are governed by electronic collisions. Therefore, a method was to be found which allowed the relative line intensities of a spectral series to be measured accurately. The highest members of the various spectral series were expected to be of very low intensity. Furthermore, because of the very small distances between adjacent lines high resolution of the spectrograph was necessary. For these reasons a grating spectrograph (Jena PGS 2) having 1300 lines per mm has been chosen the dispersion of which was 0.25 mm/Å. The spectrum produced by the PGS2-spectrograph was detected photographically. Exposure times as long as 3 hours were required in order to observe line merging.

The experimental procedure is as follows (see Fig. 3). The plasma column is observed side-on through a plane parallel quartz window. The image of the plasma section is projected to the entrance

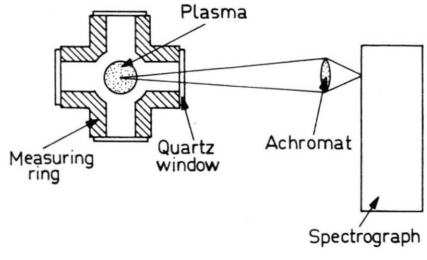

Fig. 3. Vertical cross section of the measuring ring, and optical arrangement for measuring the relative line intensities.

slit of the spectrograph by means of an achromatic quartz lens. The relative density of the photographic material as function of light intensity was calibrated using a tungsten ribbon lamp and a step filter. A typical example for a spectral series obtained in this way is shown in Fig. 4. (The axis of the plasma column is marked by a hair across the entrance slit of the spectrograph). The exposure time was 3 hours and therefore a few impurity lines appeared in the spectrum in addition to the main contamination due to hydrogen. During these very long exposure times the critical discharge parameters such as gas pres-

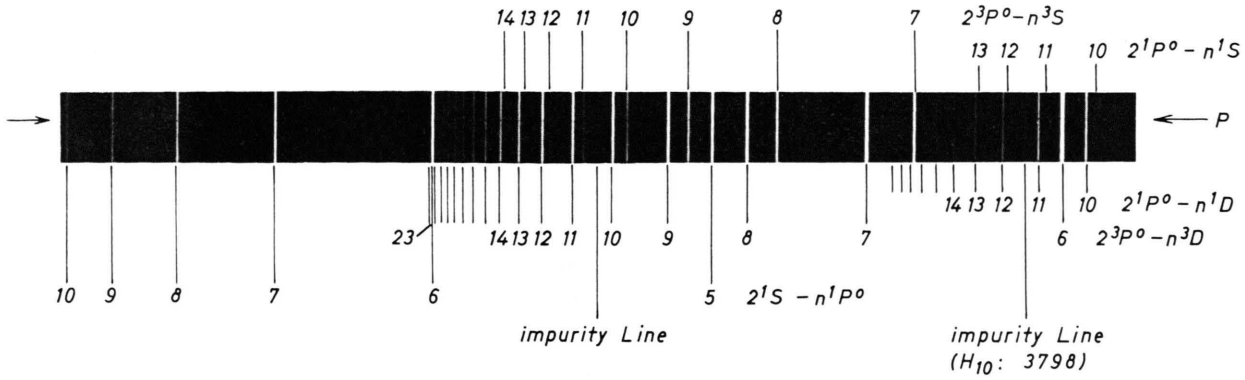

Fig. 4. Measured He I spectrum. P = position of hair across slit of spectrograph.

sure and discharge current were carefully kept constant.

The spectral series shown in Fig. 4 has been evaluated by means of a micro-densitometer. The result is presented in Fig. 5 and it can be seen that lines according to a principal quantum number up to 25 may be distinguished. This means that the electron density should be about 2.5×10^{12} cm^{-3} as may be calculated using the well known Inglis-Teller formula. Nearly the same value was found using a microwave interferometer (see section E. 3).

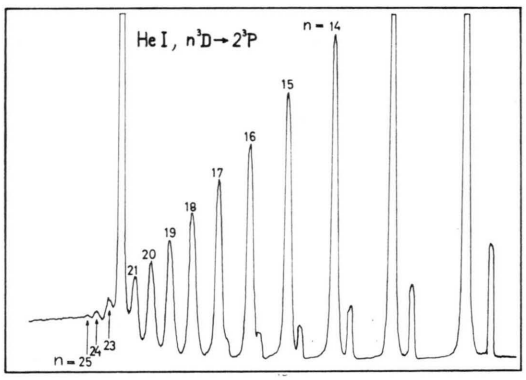

Fig. 5. Densitometer curve of the spectral series $n^3D \rightarrow 2^3P_0$ of He I.

From the calibration with the tungsten ribbon lamp it was possible to obtain a relative characteristic density curve for each wavelength desired. With the help of different exposure times of both, i.e. line spectrum and calibration spectrum, the relative line intensities of the spectral series $n^3D \rightarrow 2^3P$ from $n = 7$ up to $n = 24$ could be determined. Using transition probabilities[16,17] for the lines in question the relative population densities of the n^3D levels could be calculated from the relative line intensities. Above $n = 16$ the error bars become large due to beginning overlapping of the closely spaced lines and due to the weakness of the intensities. For $n = 22$ (see Fig. 5) the intensity could not be determined (line of transition 2^1S-6^1P superposed, see Fig. 4). Abel-inversion finally led to the radial intensities.

D. Determination of Absolute Line Intensities

The quantitative determination of absolute line intensities by means of photographic methods is difficult and time-consuming. Therefore, a photoelectric method has been used in order to avoid some of these difficulties. The principle of this method is shown in Fig. 6. The plasma column is

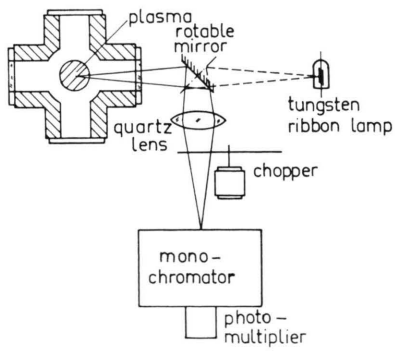

Fig. 6. Experimental arrangement for measuring absolute line intensities.

[16] Landolt-Börnstein, Zahlenwerte und Funktionen, Vol. 1, p. 260, Springer-Verlag, Berlin 1950.

[17] W. L. Wiese, M. W. Smith, and B. M. Glennon, Atomic Transition Probabilities, Vol. 1. NSRDS-NBS-4, Washington 1966.

situated at equal distance from a rotatable mirror as the tungsten ribbon lamp. The light from either the plasma or the lamp is focused on the entrance slit of a monochromator (Zeiss SPM2) after being interrupted by a rotating sector disc. The reference frequency (26 Hz) as obtained by the same disc using an illuminated photocell is fed to the reference input of a lock-in amplifier (PAR JB-5). The spectral line (or the equivalent part of the continuum of the lamp) is selected by the monochromator and detected by a photomultiplier (RCA, 1 P28) the output of which is given to the signal input terminals of the lock-in amplifier. In this way the absolute intensity of the 4471 Å line was found to be

$$J(4471) \approx 1.3 \times 10^2 \text{ erg cm}^{-3} \text{ sec}^{-1} \text{ ster}^{-1}.$$

The number densities of all excited particles which contribute to this spectral line is then given by

$$n(4471) \approx 4\pi \frac{J(4471)\,\lambda_0}{A(4471)\,h\,c} \tag{6}$$

where $A(4471)$ is the transition probability of this line and $\lambda_0 = 4.471 \times 10^{-5}$ cm it's wavelength. Inserting the numerical values one obtains

$$n(4471) \approx 1.44 \times 10^7 \text{ particles/cm}^3.$$

Dividing this value by the statistical weight $g_{n=4}=15$ gives the population density $n_4/g_4 = 9.6 \times 10^5 \text{cm}^{-3}$ of level 4^3D as indicated by the open circle for $n = 4$ on the Figs. 8a and 10a.

The population densities of the states $n = 4$ to $n = 7$ have been evaluated from photo-electric measurements. With the absolute value for state with $n = 7$ known the relative population densities of all states from $n = 7$ to $n = 24$ could be converted into absolute population densities.

The error of the *absolute* intensity measurement is estimated to be of the order of $\pm 15\,\%$. This has no influence on the temperature determination since only relative values are needed, it has an influence on the determination of the electron density, however.

E. Evaluation of Experimental Data

1. *Population densities*

We consider the population densities of excited particles in the central part of the discharge column. The logarithms of the measured absolute population densities have been plotted against the energy distance from the ionization limit (see Figs. 8, 9 and 10). The relative errors are indicated by error bars. All population densities of principal quantum numbers $n \cong 7$ to $n \cong 18$ lie on a straight line. Making use of the relation

$$k\,T_e = \frac{\Delta E_n}{\Delta \ln(n_n/g_n)} \tag{7}$$

one finds from the slope of the Boltzmann plot a temperature of

$$T_e = 1.130 \pm 100\,^\circ\text{K}.$$

We now make the assumption that atomic collisions do not influence the population densities of quantum numbers below $n = 18$ and that for all states with $18 > n > 7$ the Saha-Eggert equation in the following form

$$n_e^2 = n_n \frac{g_+ g_e}{g_n} \left(\frac{2\pi m_e k\,T_e}{h^2}\right)^{3/2} \exp\left\{-\frac{E_n}{k\,T_e}\right\} \tag{8}$$

holds. Putting into this relation the measured population densities n_n yields for the electron density the value

$$n_e = (2.80 \pm 0.45) \times 10^{12} \text{ cm}^{-3}.$$

The filling pressure of $p = 50$ m Torr leads with an assumed gas temperature of $T_a \cong 300\,^\circ$K to a neutral gas density of

$$n_0 \cong 1.4 \times 10^{15} \text{ cm}^{-3}.$$

We will see later that this density suffices to invalidate the relation (8) and that the actual electron density will probably be slightly smaller than $2.8 \times 10^{12} \text{cm}^{-3}$ due to the influence of atomic collisions upon the population densities.

Besides spectroscopic measurements Langmuir probe and microwave measurements have been performed for determining T_e and n_e. The results shall be briefly reported.

2. *Langmuir probe measurements*

The electron temperature as evaluated from a probe characteristic at identical conditions as for the spectroscopic measurements yielded a value of

$$T_e = 1.400 \pm 200\,^\circ\text{K}.$$

This agrees fairly well with the spectroscopic result (1.130 °K) if one accounts for the disturbance of the plasma by the probe and the rather large error due to uncertainties in the evaluation of the probe characteristic. At least for the conditions of the

Q-PIG one therefore finds that the pulsed Langmuir probe method should be an appropriate and convenient means to measure the electron temperature.

3. *Microwave measurements*

The electron density has been independently determined by microwave measurements. From the phase shift detected by a microwave interferometer we obtained a mean electron density (average over the diameter) of $n_e = 2.3 \times 10^{12}$ cm^{-3}. Concerning the details of the measurements the reader is referred to Ref. [14].

F. Collisional-Radiative Model for Helium I

We will now see how far the measured population densities agree with theoretical ones calculated on the basis of a collisional-radiative model.

The level system used for the calculations is the same as that one described in Refs. [18–20]: One distinguishes between the singlet-system (= X-system) and the triplet-system (= Y-system). Quantum states with principal quantum number $n \geqq 3$ are treated energetically as hydrogen-like states with the correct multiplicities and statistical weights for helium levels. States below $n = 3$ are considered as individual levels. In addition to radiative transitions and electronic collisions from and to all states we have accounted for atomic collisions.

The coupled system of rate equations to be solved is based on two times six elementary radiation and collision processes. Since Helium I has two level systems of different multiplicity the number of elementary processes is once more increased by a factor of two. We have accounted for the following processes:

1. *Electronic Ionization, and 3-body Collisional Recombination*

The processes are

$$\mathrm{He}(n) + \mathrm{e} \underset{n_e Q_n^{(e)}}{\overset{S_n^{(e)}}{\rightleftarrows}} \mathrm{He}^+ + \mathrm{e} + \mathrm{e}\,.$$

The rate coefficients are (in units cm^3/sec):

$$S_n^{(e)} = 4\pi a_0^2 \left(\frac{E_1^H}{E_n}\right)^2 f_n \zeta_n \left(\frac{2kT_e}{\pi m_e}\right)^{1/2} u_n \Psi_1(u_n, \beta_n)\,, \tag{9}$$

$$n_e Q_n^{(e)} = \frac{g_n}{2g_+} \frac{h^3}{(2\pi m_e k T_e)^{3/2}} n_e S_n^{(e)} \exp(u_n) \tag{10}$$

with

E_1^H = ionization energy of H-atom (13.6 eV),
E_n = ionization energy of level n,
$u_n = E_n/kT_e$,
$\beta_n = 1 + (Z_{eff} - 1)/(Z_{eff} + 2)$,
a_0 = first Bohr radius,
ζ_n = number of energetically equivalent electrons in shell n,
f_n = oscillator strength (normalized),
g_+, g_n = statistical weights.

The function $\Psi_1(u_n, \beta_n)$ accounts for the energy dependence of the cross sections. For a Maxwellian velocity distribution:

$$\Psi_1(x, \beta) = \int_{u=x}^{\infty} \left[\left(1 - \frac{x}{u}\right) e^{-u} \ln(1.25\beta x)\right] \mathrm{d}x\,.$$

Numerical values of Ψ_1 may be found in Refs. [4,8,9].

2. *Photo-Ionization and Radiative Recombination*

For hydrogen-like levels the rate coefficient for radiative recombination into level n is given by

$$R_n^{(e)} = 5.20 \times 10^{-14} Z_{eff}\, u_1^{3/2} G_n\, n^{-3} [-\mathrm{Ei}(u_n)] \times \exp(+u_n) \frac{\mathrm{cm}^3}{\mathrm{sec}} \tag{11}$$

with

$$u_1 = Z_{eff}^2 E_1^H / kT_e\,,$$

G_n = Gaunt factor,
$[\mathrm{Ei}(-x)]$ = logarithmic integral.

For the ground state and the levels with $n = 2$, we calculated the recombination coefficients from the absorption coefficients published in Refs. [21,22], see also Ref. [23].

Photo-ionization is expressed as a negative recombination.

3. *Electronic Excitation, and De-Excitation by Superelastic Collisions with Electrons*

The processes are

$$\mathrm{He}(k) + \mathrm{e} \underset{F_{nk}^{(e)}}{\overset{C_{kn}^{(e)}}{\rightleftarrows}} \mathrm{He}(n) + \mathrm{e}\,.$$

For optically allowed transitions the rate coefficient for excitation can be written as follows[19,23]:

[18] H. W. DRAWIN, Z. Naturforsch. **19a**, 1451 [1964].
[19] H. W. DRAWIN and F. EMARD, Report EUR-CEA-FC-534, Fontenay-aux-Roses 1970.
[20] F. EMARD, Thesis, Paris University 1971.
[21] L. GOLDBERG, Astrophys. J. **90**, 414 [1939].
[22] O. GINGERICH, Proc. 1st Harvard Smithsonian Conf. on Stellar Atmospheres, p. 17, Cambridge (Massachusetts 1964.
[23] H. W. DRAWIN, Report EUR-CEA-FC-383 (revised), Fontenay-aux-Roses 1967.

$$C_{kn}^{(e)} = 8.69 \times 10^{-8} f_{kn} Z_{\text{eff}}^{-3} \frac{u_1^{3/2}}{u_{kn}} \Psi_1(u_{kn}, \beta_{kn}) \frac{\text{cm}^3}{\text{sec}}, \tag{12}$$

$$F_{nk}^{(e)} = \frac{g_k}{g_n} C_{kn}^{(e)} \exp(u_{nk}) \tag{13}$$

with

f_{kn} = absorption oscillator strength for transition $k \to n$,

$u_{kn} = |u_k - u_n| = |E_k - E_n|/k T_e$.

The function Ψ_1 has the same meaning as in Eq. (9), with other arguments, however.

In addition, forbidden transitions without and with a change in multiplicity have been taken into account. The corresponding rate coefficients used for the calculations may be found in Ref. [19].

4. Spontaneous De-Excitation, and Excitation by Radiative Absorption

The spontaneous transition probabilities A_{kn} have been taken from Ref [17]. For the very highly excited levels we applied the asymptotic formula for hydrogen-like transitions[16]. Radiative absorption has been treated as a negative spontaneous deexcitation.

5. Ionization by Collisions with Heavy Particles in the Ground State 1^1S_0, and 3-body Collisional Recombination

The corresponding processes are:

$$\text{He}(n) + \text{He}(1^1S_0) \underset{n_e Q_n^{(0)}}{\overset{S_n^{(0)}}{\rightleftarrows}} \text{He}^+(1^2S_{1/2}) + \text{He}(1^1S_0) + \text{e}.$$

The rate coefficient for ionization writes[24]

$$S_n^{(0)} = 32\pi a_0^2 \left(\frac{E_1^H}{E_n}\right)^2 \zeta_n f_n \left(\frac{k T_a}{\pi m_a}\right)^{1/2} \times \frac{m_e m_a}{m_H (m_e + m_a)} \Psi_{m_a}(w_n) \tag{14}$$

with

m_H = mass of H atoms,

m_a = mass of He atoms,

$w_n = E_n/k T_a$.

$$\Psi_{m_a}(w_n) = \left(1 + \frac{2}{w_n}\right)\left(\frac{1}{1 + (2 m_e/(m_a + m_e)\, w_n)^2}\right) \times \exp\{-w_n\}.$$

For the recombination coefficient follows

$$n_e Q_n^{(0)} = \frac{g_n}{2 g_+} \left(\frac{m_a + m_e}{m_e m_a}\right)^{3/2} \frac{h^3}{(2\pi k)^{3/2}} \frac{n_e S_n^{(0)}}{T_a^{1/2} T_e} \times \exp(-u_n + 2 u_n^{1/2} w_n^{1/2}) \tag{15}$$

which depends on T_e and T_a. If $T_e = T_a$ Eq. (15) yields the equilibrium relation (detailed balancing).

6. Excitation of Level n by Collisions of Ground State Particles (1^1S_0) with Lower Lying Levels $k (k < n)$, and the Inverse Process

The following reactions are considered

$$\text{He}(k) + \text{He}(1^1S_0) \underset{F_{nk}^{(0)}}{\overset{C_{kn}^{(0)}}{\rightleftarrows}} \text{He}(n) + \text{He}(1^1S_0).$$

In analogy to Eq. (14) we write for the excitation coefficient

$$C_{kn}^{(0)} = 32\pi a_0^2 \left(\frac{E_1^H}{E_{kn}}\right)^2 f_{kn} \left(\frac{k T_a}{\pi m_a}\right)^{1/2} \frac{m_e m_a}{m_H (m_a + m_e)} \times \Psi_{m_a}(w_{kn}) \tag{16}$$

with

$$w_{kn} = |w_k - w_n| = |E_k - E_n|/k T_a.$$

Application of the method of detailed balancing yields for the rate coefficient for de-excitation the expression

$$F_{nk}^{(0)} = \frac{g_k}{g_n} C_{kn}^{(0)} \exp(w_{kn}). \tag{17}$$

It is to be noted that all collision coefficients are based on a Maxwellian velocity distribution of the colliding particles.

We now consider the Zero-order moment of the Boltzmann collision equation for the n-th state:

$$\frac{\partial n_n}{\partial t} + \nabla \cdot (n_n \langle \boldsymbol{v}_n \rangle) = \left(\frac{\partial n_n}{\partial t}\right)_{\text{collision, radiation}}. \tag{18}$$

The first term on the left-hand side becomes equal to zero, since the plasma in the Q-PIG is a steady-state plasma. For the second term we make the assumption that it is small compared to the collisional-radiative term on the right-hand side in the special case of excited levels. This enables us to treat the excited particles as a separate fluid coupled with the electron-ion fluid and with the fluid of ground state particles by the proper diffusion equations:

$$\nabla \cdot (n_e \langle \boldsymbol{v}_e \rangle) = \left(\frac{\partial n_e}{\partial t}\right)_{\substack{\text{inelastic and} \\ \text{elastic collisions}}}, \tag{19a}$$

$$\nabla \cdot (n_0 \langle \boldsymbol{v}_0 \rangle) = \left(\frac{\partial n_a}{\partial t}\right)_{\substack{\text{inelastic and} \\ \text{elastic collisions}}}. \tag{19b}$$

For a low-temperature plasma $n_e = n_+$ holds. The first equation describes ambipolar diffusion and spatial recombination relaxation. The second equation describes diffusion of helium ground state particles (index odd) and spatial ionization relaxation. When $n_e(r)$, $n_0(r)$, $T_e(r)$ and $T_a(r)$ are known (for instance from a solution of the diffusion equa-

[24] H. W. Drawin, Z. Physik **211**, 404 [1968].

tions and/or from measurements) the *excited* state populations can be calculated from a coupled system of rate equations of type (18) with the terms on the left-hand side equal to zero. Thus, the collisional-radiative term of state k can be put into the following form:

$$0 = \left(\frac{\partial n_k}{\partial t}\right)_{\substack{\text{inelastic collisions,}\\ \text{radiation}}} = \sum_{n=1}^{p} (c_{kn} + c'_{kn})\, n_n + \alpha_k + \alpha'_k\,, \quad k = 1, \ldots, p\,, \tag{22}$$

with the highest still bound state p given by

$$p \cong \left(\frac{Z\langle d_+\rangle}{a_0}\right)^{1/2} = 1.08 \times 10^4 Z^{1/2} n_+^{-1/6}\,.$$

$\langle d_+\rangle$ is the mean distance between charged particles, Z the charge number felt by the optical electron, a_0 the first Bohr radius, n_+ the number density of ions.

There exists an equal number of equations for the X- and Y-system. The coefficients of Eq. (22) are related to the rate coefficients by the following equations:

$$\left.\begin{aligned} c_{kn} &= \Lambda_{kn} A_{kn} + n_e F^{(e)}_{kn} \\ c'_{kn} &= n_0 F^{(0)}_{kn} \end{aligned}\right\} \text{for} \quad k < n\,, \tag{23}$$

$$\left.\begin{aligned} c_{kn} &= n_e C^{(e)}_{kn} \\ c'_{kn} &= n_0 C^{(0)}_{kn} \end{aligned}\right\} \text{for} \quad k > n\,, \tag{24}$$

$$\left.\begin{aligned} c_{kn} &= -\left[\sum_{k=1}^{n-1} c_{kn} + \sum_{k=n+1}^{p} c_{kn} + n_e S^{(e)}_n\right] \\ c'_{kn} &= -\left[\sum_{k=1}^{n-1} c'_{kn} + \sum_{k=n+1}^{p} c'_{kn} + n_0 S^{(0)}_n\right] \end{aligned}\right\} \text{for} \quad k = n\,, \tag{25}$$

$$\left.\begin{aligned} \alpha_n &= n_+ n_e (\Lambda_n R^{(e)}_n + n_e Q^{(e)}_n) \\ \alpha'_n &= n_+ n_e n_0 Q^{(0)}_n \end{aligned}\right\} \text{for} \quad k = n\,. \tag{26}$$

The coefficients Λ_i and Λ_{kn} are reduction coefficients due to radiative absorption[8] with

$$0 \leqq \Lambda_i \leqq 1\,, \quad 0 \leqq \Lambda_{kn} \leqq 1\,.$$

By solving the coupled system of rate equations one obtains the number densities of the excited states. In the numerical calculations quantum states up to $n = 25$ have been taken into account.

G. Numerical Results, Comparison with Experiment

1. No atomic collisions

In the numerical evaluation of the coupled system of rate equations we make first the assumption that atomic collisions do not occur, compared to electron-atom and electron-ion collisions. This is equivalent with the non-existence of the primed terms in the coupled system of Eqs. (22). Thus, by putting all c'_{kn} and α'_n equal to zero we can solve (22) for the number densities n_n when n_e and T_e are given. An example of the calculated population densities of the n^3D-levels is shown in Figs. 7a, b for

$$n_e = 2 \times 10^{12}\ \text{cm}^{-3}$$

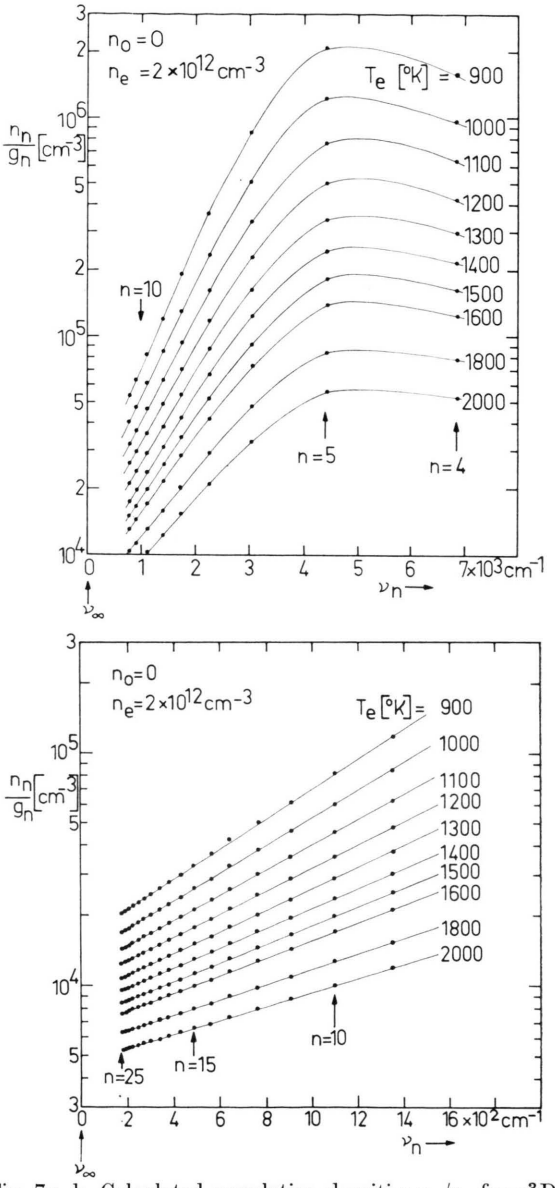

Fig. 7a, b. Calculated population densities n_n/g_n for n^3D-levels versus ionization energy ν_n. n_0 atomic collisions, electron density $n_e = 2 \times 10^{12}\ \text{cm}^{-3}$. All resonance lines are assumed to be optically thick, all other lines, and all recombination continua optically thin.

with T_e as a parameter. ν_n represents the energy difference from the ionization limit at $\nu_\infty = 0$. For $n \geqq 6$ all values lie on a straight line. The slope yields the electron temperature in agreement with the theoretical predictions when atomic collisions do not occur. For all states with principal quantum numbers $n > i$ [with i given by Eq. (2)] the Saha-Eggert eq. in the form of Eq. (8) is valid.

2. *Atomic collisions are effective*

We now assume that the primed terms of (22) are not equal to zero, i.e. we make the assumption that atomic collisions can have an influence on the solutions of Eqs. (22). By chosing values for n_e, T_e, n_0 and T_a one can solve for the population densities n_n. Figs. 8a, b show the calculated population densities of the n^3D-levels for

$$n_0 = 1 \times 10^{15}\,\mathrm{cm}^{-3}, \quad T_a = 300\,^\circ\mathrm{K}\,,$$
$$n_e = 2 \times 10^{12}\,\mathrm{cm}^{-3}$$

with T_e as a parameter.

One sees that for principal quantum numbers $18 \geqq n \geqq 6$ all values lie on a straight line the slope of which leads to the electron temperature. For $n > 18$ one obtains a slight change of the slope for all curves. The slope increases with increasing quantum number. At $n = 25$ — where line merging begins — the population densities have not yet reached a new equilibration temperature (which should be equal to the gas temperature T_a at very high atom densities).

There is another important difference between the curves given in Figs. 7a, b and Figs. 8a, b which shall be discussed now. Consider the parameters and the population densities of these figures. Concerning the plasma parameters, the only difference between them is that Figs. 8a, b additionally account for atom-atom collisions whereas the electron density is the same for both the Figs. 7a, b and Figs. 8a, b. Atomic collisions obviously increase the *absolute* values of the population densities of levels having low and medium principal quantum numbers ** — compared to the population densities in which

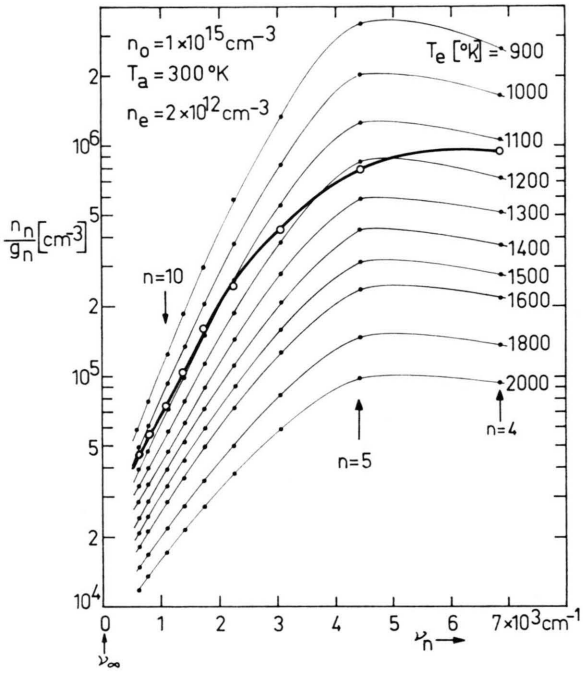

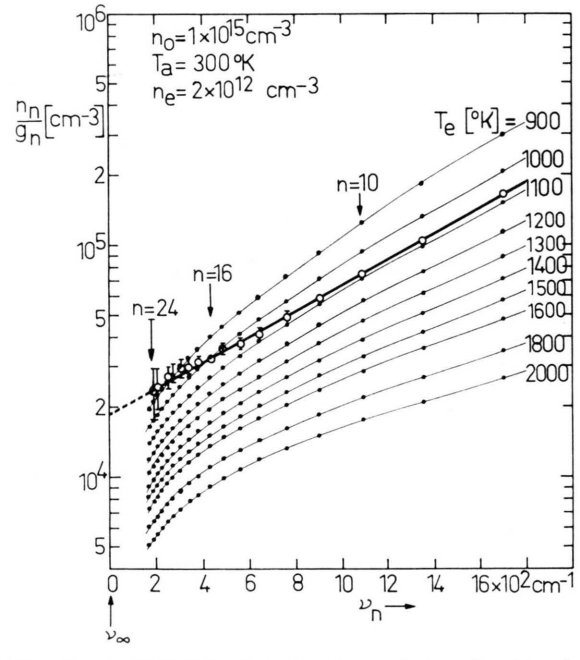

Figs. 8a, b. *Full dots*: Calculated population densities for n^3D-levels. Electronic and atomic collisions are assumed to be efficient. $n_0 = 1 \times 10^{15}\,\mathrm{cm}^{-3}$, $T_a = 300\,^\circ\mathrm{K}$, $n_e = 2 \times 10^{12}\,\mathrm{cm}^{-3}$. All resonance lines are assumed to be optically thick.
Open circles: Measured population densities.

** This only holds if $T_a < T_e$. When $T_a = T_e$ the population densities are the same without and with atomic collisions. This follows immediately from the general relations for thermal equilibrium. It has also been checked numerically by solving the coupled system of Equations for equal atom and electron temperatures. In this case the population densities were the same without and with atomic collisions (see also Ref. [12]) as it must be.

atomic collisions are absent — although the corresponding population densities follow *relatively* to each other the electron temperature. Only at very high quantum numbers the relative population densities begin to follow the gas temperature. Physically this can be understood when one considers the different types of electronic and atomic collisions: At low and medium principal quantum numbers n (i.e. for $j > n > i$) only electron collisions are effective in equipartionning the levels relative to each other, the influence of atomic collisions is negligibly small. Thus, the relative population densities have necessarily to follow T_e. However, when $T_a < T_e$ atomic collisions increase the general recombination rate and, thus, contribute to an increase of the absolute population densities relative to those calculated from the Saha-Eggert Equation in the form of Eq. (8). (See also Ref. [12].)

At very high quantum numbers n (i.e. for $n > j$) mainly atomic collisions equilibrate the population densities relative to each other, electronic collisions are less effective. Thus, these population densities must follow a temperature which — in the limit of very high atomic densities — corresponds to the gas temperature.

It follows from this that an evaluation of the Boltzmann plot at low and medium quantum number n will always yield T_e. However, when $T_a \neq T_e$ and $n_0 \gg n_e$ the electron density can not be calculated from the Saha-Eggert Equation in the form as given by Eq. (8), it has to be replaced by a more general equation containing T_a and T_e.

3. *Comparison with Experiment*

In order to find the solutions which best match the measured population densities we calculated the population densities for different values n_e and T_e with n_0 and T_a fixed. Fig. 9 shows the result for $n_e = 3 \times 10^{12}$ cm^{-3}. All values are much to high compared to the experimental values. The experimental population densities agree best with the solutions of the coupled system of rate equations when the following parameters are taken:

$$n_0 = 1.5 \times 10^{15}\ \text{cm}^{-3}, \quad T_a = 300\ ^\circ\text{K},$$
$$n_e = 2.42 \times 10^{12}\ \text{cm}^{-3}, \quad T_e = 1220\ ^\circ\text{K}$$

as can be seen from Figs. 10a, b.

When we would have compared the experimental values with the numerical solutions without taking into account atomic collisions we would have obtained a best match of experimental and theoretical population densities for $n_e = 2.8 \times 10^{12}$ cm^{-3} and $T_e = 1150\ ^\circ$K. One sees that the influence of atomic collisions thus decreases the electron density compared to that one calculated from the Saha-Eggert Equation in the form of Eq. (8) for known values of n_n and T_e. The value of 2.42×10^{12} cm^{-3} is in much better agreement with that one obtained from microwave measurements (2.3×10^{12} cm^{-3}) than with that one derived from Eq. (8). It may be considered as an additional indication that Eq. (8) is indeed not applicable when atomic collisions are important in populating highly excited levels.

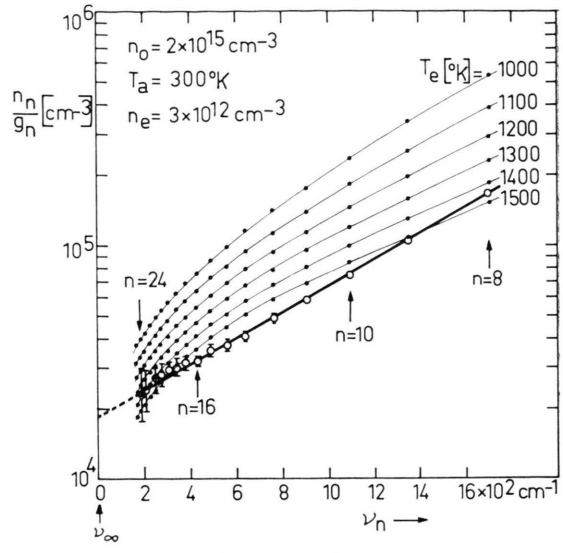

Fig. 9. As Figs. 8a, b, but with other values for n_0 and n_e.

Due to the theoretical calculation the slope of the Boltzmann plot should be larger for states with $n > j$ than for those with $n < j$, thus indicating that the population densities begin to equilibrate towards a new "equilibration temperature". As can be seen from the figures, the experimental values do not permit a decision on whether such a change of the slope takes place or not. The experimental error bars are much too large. The proof that this effect exists is, thus, still pending.

H. Remarks on Production and Loss of Charged Particles

The measurements yield extremely low electron temperatures ($kT_e \approx 0.1$ eV). If this temperature were really the electron temperature, the Q-PIG plasma could not exist. To understand this situation

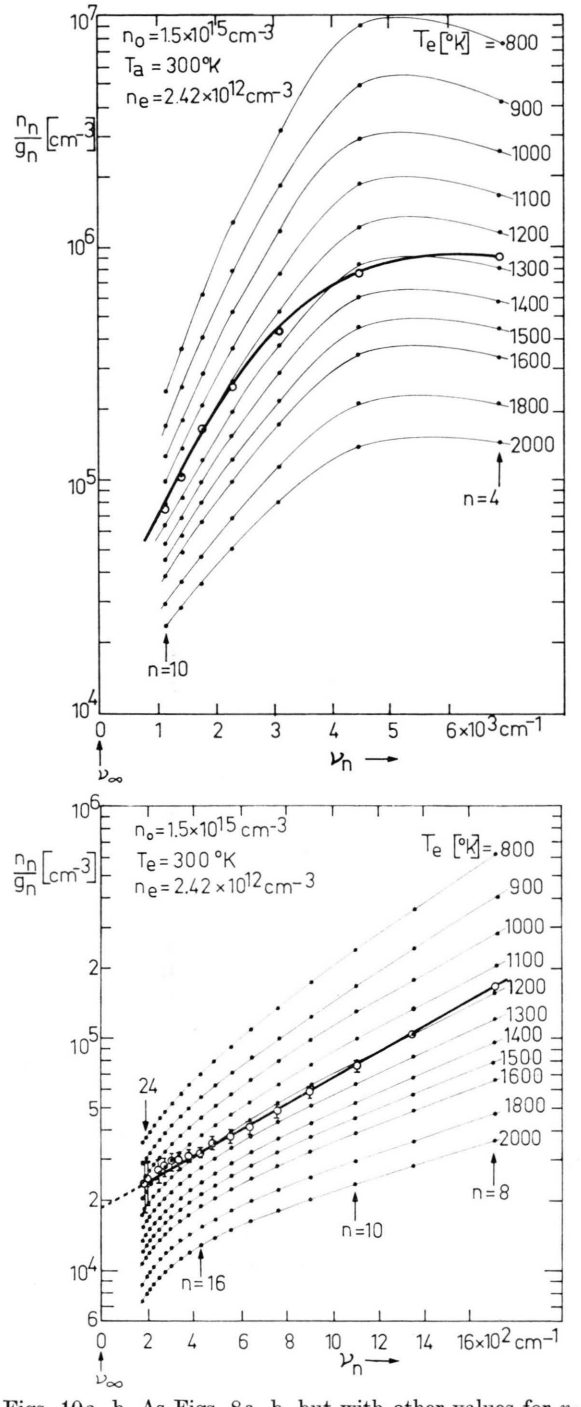

Figs. 10a, b. As Figs. 8a, b, but with other values for n_0 and n_e.

we have to compare the loss rates with the rates for particle production.

For the given experimental parameters one obtains a volume recombination coefficient[25] of $\alpha \cong 3.5 \times 10^{10}\,cm^3/sec$ which leads to a volume recombination rate of

$$(\partial n_e/\partial t)_{recomb} = \alpha n_e^2 = 2.2 \times 10^{15}\,cm^{-3}\,sec^{-1} \quad (27)$$

for a plasma which is optically thick towards the resonance lines.

The particle loss due to classical diffusion leads to a value of

$$(\partial n_e/\partial t)_{diff} \approx 1 \times 10^{16}\,cm^{-3}\,sec^{-1}. \quad (28)$$

On the other hand, the particle production rate is determined by number and mean energy of the secondary electrons produced at the cathode surface by ion bombardment[14]. Because of the confining electrode geometry of the Q-PIG and the magnetic field these electrons are trapped within the plasma volume until having lost most of their initial energy. Assuming that this energy were consumed completely by ionizing collisions, we may find an upper limit for the production rate. At a discharge current of 160 mA the average number of secondaries, q_e, produced per sec and per cm^2 of the cathode surface was calculated to be approximately[14] $10^{16} cm^{-2} sec^{-1}$. The operation voltage was about 500 V and therefore the initial energy E_0^* of the electrons leaving the cathode fall region should be of this order as well: $E_0^* \approx 500$ eV. Since the ionization energy of the neutral helium, E_{ion}, is about 25 eV, the maximum number of ionizing collisions of each secondary electron is about 20. Averaging the whole number of ionizations per sec over the plasma volume yields:

$$\left\langle\left(\frac{\partial n_+}{\partial t}\right)\right\rangle = \frac{2 q_e}{L}\frac{E_0^*}{E_{ion}} \approx 0.8 \times 10^{16}\,cm^{-3}\,sec^{-1}. \quad (29)$$

where the factor 2 accounts for the two emitting cathodes and L is the length of the plasma (L = 50 cm). This value approximately agrees with the loss rate due to diffusion and is one order of magnitude larger than the volume recombination rate. One has to conclude that for $n_e = 2.5 \times 10^{12}\,cm^{-3}$ and $T_e = 1.2 \times 10^3$ °K the plasma in the Q-PIG device is still diffusion dominated.

As the recombination rate increases like n_e^3 and the diffusion rate like n_e the Q-PIG plasma will come into the regime of volume recombination for electron densities larger than approximately $10^{13}\,cm^{-3}$ provided anormal diffusion losses remain small.

Acknowledgements

We thank Miss F. Emard for having written the computer programme. The numerical calculations have been performed on the IBM electronic computer 360/75 at the Centre d'Etudes Nucléaires, Saclay.

[25] H. W. Drawin and F. Emard, (to be published).